Alkaline electrolysers with enhanced durability

ENDURE

[AST protocols for AEL electrodes]

(Deliverable D4.1)

The project is supported by the Clean Hydrogen Partnership and its members		
PU	Public, fully open	x
SEN	Sensitive, limited under the conditions of the Grant Agreement	☐
Classified R-UE/EU-R	EU RESTRICTED under the Commission Decision No2015/444	☐
Classified C-UE/EU-C	EU CONFIDENTIAL under the Commission Decision No2015/444	☐
Classified S-UE/EU-S	EU SECRET under the Commission Decision No2015/444	☐

Co-funded by the European Union. Views and opinions expressed are however those of the author(s) only and do not necessarily reflect those of the European Union or Clean Hydrogen JU. Neither the European Union nor the granting authority can be held responsible for them.

NOTICES

For information, please contact the project coordinator, Mari Šavel, e-mail: mari.savel@stargatehydrogen.com. This document is intended to fulfil the contractual obligations of the ENDURE project, which has received funding from the Clean Hydrogen Partnership and its members, concerning deliverable D4.1 described in contract 101137925.

Authors

Tobias Ludwig

Reviewer(s)

Anna Katharina Müller

Susanne Holmin

Table of revisions

Version	Date	Description and reason	Author	Affected sections
V0.1	23.01.2026	1st Draft	Tobias Ludwig	All sections
V0.2	03.02.2026	Review	Anna Katharina Müller	All sections
V0.3	09.02.2026	Review	Susanne Holmin	All sections
V1.0	11.02.2026	Final draft	Tobias Ludwig	All sections
V1.1	24.02.2026	Figure correction	Tobias Ludwig	Table 9

Clean Hydrogen Partnership Co-funded by the European Union

The project is supported by the Clean Hydrogen Partnership and its members

List of Partners

Stargate Hydrogen Solutions OÜ (Stargate)
Fraunhofer-Institut für Fertigungstechnik und Angewandte Materialforschung (IFAM)
Zentrum für Sonnenenergie- und Wasserstoff-Forschung Baden-Württemberg (ZSW)
Fundación para el Desarrollo de las Nuevas Tecnologías del Hidrógeno en Aragón (FHa)
Permascand AB (Permascand)
Université catholique de Louvain (UCLouvain)

Clean Hydrogen Partnership Co-funded by the European Union
The project is supported by the Clean Hydrogen Partnership and its members

List of Abbreviations

AEL	Alkaline electrolysis
AST	Accelerated stress test
BoL	Beginning of life
CDL	Capacitive double-layer capacitance
CE	Counter electrode
EoL	End of life
HC	High currents
Imp	Impurities
JRC	Joint Research community
OCP	Open circuit potential
RE	Reference electrode
RHE	Reversible hydrogen electrode
T_{nom}	Nominal temperature
WE	Working electrode
WP	Work package

List of Figures

List of Tables

Clean Hydrogen Partnership Co-funded by the European Union
The project is supported by the Clean Hydrogen Partnership and its members

Table of Contents

Clean Hydrogen Partnership Co-funded by the European Union
The project is supported by the Clean Hydrogen Partnership and its members

1 Objectives

The objective of this document is to deliver a broad approach of accelerated stress tests (AST) for electrodes of alkaline electrolysis in as much detail as possible for the research community. The AST protocols are intended to simulate the long-term degradation of electrodes occurring during real operation of alkaline electrolysers, while inducing these effects over a significantly shorter test duration.

By following the instructed test profiles research partners can evaluate the performance and stability of electrodes in single-cell setups based on characteristic stressors. The addressed stressors are dynamic operation, excessive load, repetitive starts and stops, reverse currents and electrolyte impurities.

The JRC states that “in future, other load profiles, once validated, can be benchmarked against and possibly update and/or replace this set” (Tsotridis and Pilenga 2021). Building on this perspective, we aim to advance the JRC’s approaches for accelerated stress testing (AST) with a specific focus on electrodes, while integrating and extending the testing methodologies established in their work.

2 Approach

The accelerated stress tests (ASTs) developed in this work are designed for half-cell testing of electrodes used in alkaline electrolysis. In this configuration, the electrode under evaluation is defined as the working electrode (WE). A reference electrode (RE) with a well-defined and stable potential—preferably a reversible hydrogen electrode (RHE)—is used to measure the WE potential. A counter electrode (CE) completes the electrical circuit but is not considered in the performance evaluation.

The specific half-cell configuration is not further defined for the AST methods addressed in this work. However, in order to reliably perform these tests, the half-cell setup must meet the following requirements:

- Maintaining a stable and homogeneous temperature throughout the cell
- Ensuring a precisely defined geometric area of the working electrode
- Providing the measurement accuracy for temperature, current, and potential as required by the JRC (see JRC 122565 (Tsotridis and Pilenga 2021) , Table 14)
- Maintaining a stable KOH concentration within the test cell for the entire test duration (> 50 h)
- Prevention of the introduction of foreign elements and impurities into the electrolyte

ASTs developed for electrode evaluation are most suitably performed in a half-cell setup, as this configuration enables precise assessment of changes in electrode performance and stability while minimizing external influences. Nevertheless, most of the ASTs described in this work can also be implemented at the full-cell level, where the cell voltage and current between anode and cathode are evaluated without reference to an individual electrode potential. Wherever full-cell operation is suitable for a given AST, this is explicitly stated.

For the complete characterisation of an electrode within a given AST method, a uniform procedure has been developed, which is applied consistently across all ASTs. The first step is the activation and conditioning of the electrode according to the electrode-specific requirements. The objective of conditioning is to establish stable operating conditions, defined by a change in electrode overpotential of less than 0.2 mV/h.

Clean Hydrogen Partnership Co-funded by the European Union The project is supported by the Clean Hydrogen Partnership and its members

This is followed by a pre-characterisation protocol (see Chapter 2.1), which assesses the electrode behaviour at the beginning of life (BoL). After completion of the pre-characterisation, the AST is performed. The AST protocols are described in detail in Chapter 3 and typically last approximately 48 hours.

Following the AST, a post-characterisation is carried out to evaluate the electrode behaviour at the end of life (EoL). The pre- and post-characterisation steps follow the same protocol (see Chapter 2.1). This allows a precise assessment of the AST's impact on electrode performance by directly comparing the BoL and EoL characterisation results. The methodology for deriving performance values from pre- and post-characterization data is described in Chapter 4.

For each AST study, the nominal temperature, KOH concentration, current density, and geometric electrode area must be defined based on the electrode's operating window and the capabilities of the test setup. In our experimental approach, the following nominal parameters were selected:

$$i_{nom} = 600\ mA/cm^2$$
$$\omega_{KOH} = 30\ wt.\%\ (\pm 2\ wt.\%)$$
$$T_{nom} = 70\ °C\ (\pm 1\ °C)$$
$$A_{electrode} = 3\ cm^2$$

If the operating window or performance characteristics of the electrode under investigation are not well known, it is advisable to adjust these nominal values accordingly.

To evaluate the electrode's performance without any stressor compared to the outcome of the ASTs a reference test is performed for every study on an electrode which maintains the nominal parameters described above for 48 h also embedded in a pre- and post-characterisation (see chapter 2.2).

After the electrochemical post-characterisation, a post-mortem analysis is conducted to assess potential changes induced by the AST. This analysis may address the following aspects: the material composition of the electrode surface, alterations in surface morphology, catalyst loading, damage to the electrode surface, and catalyst layer thickness.

The following figure presents a schematic overview of the general AST approach used in this work, as described in the preceding section.

Clean Hydrogen Partnership Co-funded by the European Union
The project is supported by the Clean Hydrogen Partnership and its members

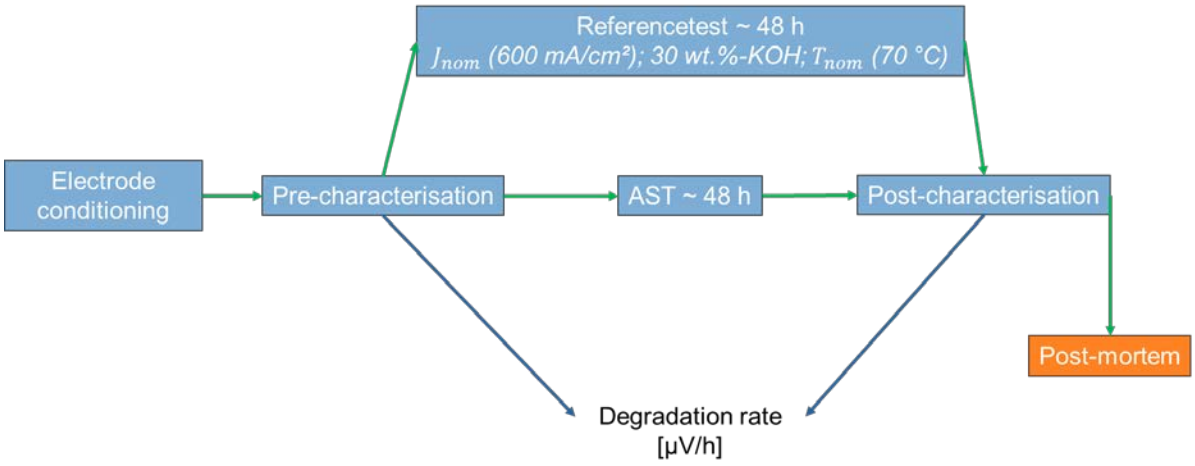

Figure 1: schematic overview of the AST approach

The experimental investigations in this work focus on cathode testing, reflecting the emphasis of the ENDURE project to date and the detailed cathode development carried out within Work Package 2. While most of the ASTs described herein are, in principle, also applicable to anode testing, their experimental validation in this study is limited to a specific Raney nickel cathode type. The suitability of each AST for cathode or anode application is explicitly stated in the respective protocol descriptions (see chapter 3).

2.1 Characterisation profile

The characterisation protocol applied within the AST framework of this work is aligned with the harmonised half-cell testing protocol described in deliverable 1.2, *"Report on Harmonised Test Protocols Adopted for ENDURE" (Martínez et al. 2024).* This protocol encompasses all key methods required for a comprehensive electrode evaluation, including conditioning, Tafel analysis, electrochemical impedance spectroscopy, constant-current operation, and cyclic voltammetry for the determination of the electrode capacitive double-layer capacitance (CDL). The same protocol is applied both before and after the AST, serving as the pre- and post-characterisation procedure (see Figure 1).

The test protocol consists of the following steps:

- **Step 1:** Conditioning η_{500} (5 h) - overpotential towards HER/OER for 5 h at 500 A cm^{-2}
    - Overpotential IR compensated
    - **Step 1.2:** Relaxation for 5 minutes at open circuit potential (OCP)
        - ➔ Comment: The conditioning might change depending on the electrode

- **Step 2:** Tafel plot / polarization curve (ascending) up to 500 A $cm^{-2}$with stepwise galvanostatic measurements between 0.1 to 500 mA cm^{-2}. (See Table 1)
    - Overpotential IR compensated

- **Step 3:** Impedance spectroscopy at various overpotentials between η=300 - 0 mV vs HER/OER (potentiostatic) or between j=0 - 100 mA cm^{-2} (galvanostatic) in a frequency range of 300 kHz – 0.1 Hz

Clean Hydrogen Partnership Co-funded by the European Union
The project is supported by the Clean Hydrogen Partnership and its members

- **Specific suggestion:**
  Galvanostatic EIS
  DC current: 40 mA cm^{-2}
  AC current: 6 mA cm^{-2} (15 % of DC)
  Initial frequency: 300 kHz
  Final frequency: 0.1 Hz
  Points/decade: 10

- **Step 4:** η_{1000}(5 h): overpotential towards HER/OER for 5 h at 1000 mA cm^{-2}
  - Overpotential IR compensated
  - **Step 4.1:** Relaxation for 5 minutes at OCP

- **Step 5:** Tafel plot / polarization curve (ascending) up to 1000 mA cm^{-2} with stepwise galvanostatic measurements between 0.1 to 1000 $mAcm^{-2}$. (See Table 1)
  - Overpotential IR compensated

- **Step 6:** Impedance spectroscopy at various overpotentials between η=300 - 0 mV vs HER/OER (potentiostatic) or between j=0 - 100 mA cm^{-2} (galvanostatic) in a frequency range of 300 kHz – 0.1 Hz
  - **Specific suggestion:**
    Galvanostatic EIS
    DC current: 40 mA cm^{-2}
    AC current: 6 mA cm^{-2} (15 % of DC)
    Initial frequency: 300 kHz
    Final frequency: 0.1 Hz
    Points/decade: 10

- **Step 7:** Cyclic voltammetry +50 mV to -50 mV vs. OCP or around a specific non-faradaic potential (e.g., +0.4 V vs RHE) with varying sweep rate (10 – 1000 mV s^{-1}) (a pre-treatment step is sometimes used before step 7).

The polarisation curves will be performed with stepwise galvanostatic measurements. Each step will be held for a minimum of 30 seconds (dwell time) with a sampling rate of 1 point/second. The approach used for recording the polarisation curve is inspired by the JRC guideline (Method B) *"EU Harmonised Polarisation Curve Test Method for Low-Temperature Water Electrolysis."* (Malkow et al. 2018). Compared to the original method, a higher number of current steps is applied in the low current density region in order to achieve increased resolution for the subsequent Tafel analysis. The following steps will be performed (Table 1):

Table 1: Specification of the steps for the polarization curve

Step	1	2	3	4	5	6	7	8	9	10
mA/cm^2	0.1	0.16	0.25	0.4	0.63	1	1.26	1.58	2	2.51
Step	**11**	**12**	**13**	**14**	**15**	**16**	**17**	**18**	**19**	**20**
mA/cm^2	3.16	3.98	5	6.31	7.94	10	12.59	15.85	19.95	25.12
Step	**21**	**22**	**23**	**24**	**25**	**26**	**27**	**28**	**29**	**30**

Clean Hydrogen Partnership Co-funded by the European Union
The project is supported by the Clean Hydrogen Partnership and its members

mA/cm^2	31.62	39.81	50.12	63.1	79.43	100	112.2	125.9	141.25	158.5
Step	31	32	33	34	35	36	37	38	39	40
mA/cm^2	177.8	200	223.9	251.2	281.8	316.23	354.81	398.81	446.68	500
Step	41	42	43	44	45					
mA/cm^2	600	700	800	900	1000					

2.2 Reference profile

The reference profile consists of a constant-current operation applied to the electrode for a duration of 48 h. It reflects the electrode behaviour under steady electrolysis conditions without the influence of additional stressors. For each electrode AST study, the reference profile is conducted at least two times using freshly prepared electrodes. As with all profiles presented in this work, the reference profile is embedded within a pre- and post-characterisation procedure as described in Chapter 2.1.

The primary purpose of the reference profile is to enable reliable comparison between electrodes subjected to AST conditions and those operated under constant-load conditions. This comparison allows identification of stressors that have a significant impact on electrode degradation, as opposed to effects that do not exceed those observed under steady operation. In addition, evaluation of the reference profiles provides insight into the reproducibility of both the electrode fabrication and the test setup.

Electrodes with inhomogeneous catalyst coatings may exhibit increased variability in performance. Deviations between reference profile results may therefore arise from non-uniform catalytic surface structures or from systematic variations within the test setup. Based on experimental experience, deviations of less than 10 mV between reference profile measurements of the same electrode type indicate very good reproducibility, deviations between 10 and 25 mV indicate moderate reproducibility, and deviations exceeding 25 mV are considered indicative of poor reproducibility.

This profile is valid for both anodes and cathodes and may also be performed in full-cell setups.

The following table summarises the operating conditions and protocol applied for the reference profile.

Table 2: detailed description of reference profile

Temperature [°C]	**KOH concentration** [wt. %]	**Electrolyte flow** [ml/(min*cm²)]	**Operation mode**	**Profile suitable for**
70	30	natural convection	steady	Anode & Cathode
Step	**Sequence**	**Function**	**Current density [mA/cm²]**	**Duration [s]**
1	OCP	start	0	20
2	Galvanostatic	constant current	600	172800
3	OCP	end	0	20

Clean Hydrogen Partnership Co-funded by the European Union
The project is supported by the Clean Hydrogen Partnership and its members

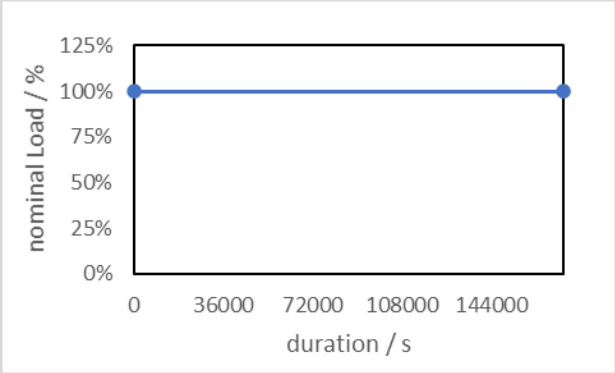

3 Cell level accelerated stress test protocols for AEL electrodes

In the following section the AST profiles applied and developed in this work are presented.

3.1 Long-term constant load profile

While ASTs are designed to accelerate electrode degradation by applying high-frequency stressors over short time periods, a long-term investigation under steady operating conditions is required to assess degradation effects arising from prolonged electrolysis. In particular, the continuous evolution of hydrogen or oxygen gas bubbles at the electrode surface cannot be fully reproduced by AST protocols. For this reason, long-term constant-load testing is considered an essential component of each electrode AST study.

The long-term constant-load profile is operated at the same constant nominal conditions as the reference profile and is conducted for a minimum duration of 1000 operating hours. For practical reasons, test interruptions due to setup adjustments, unforeseen shutdowns, or electrolyte (lye) corrections are permitted within this profile. This also includes planned shutdowns during non-operational periods, such as overnight stops, where required to comply with laboratory safety regulations.

Following any intentional or unintentional shutdown, the current is increased from open-circuit conditions to its nominal value using a controlled current ramp of 5 mA cm^{-2} s^{-1} after heating the cell setup from ambient temperature to its nominal temperature T_{nom} (70 °C) while the cell is without any load. This procedure ensures a gentle restart of operation and avoids excessive stress associated with rapid current application. This test profile is suitable for cathodes and anodes and can be performed in full cell setups. Table 3 summarises the detailed long-term constant-load protocol; steps 2.1 to 2.4 are only applicable in the event of a shutdown.

Clean Hydrogen Partnership Co-funded by the European Union
The project is supported by the Clean Hydrogen Partnership and its members

Table 3: detailed description of long-term constant load profile

Temperature [°C]	KOH concentration [wt. %]	Electrolyte flow [ml/(min*cm²)]	Operation mode	Profile suitable for
70	30	natural convection	steady	Anode & Cathode
Step	**Sequence**	**Function**	**parameters**	**Duration [s]**
1	OCP	start	0 mA/cm²	20
2	Galvanostatic	constant current	600 mA/cm²	3600000
2.1	OCP	shutdown	0 mA/cm²	-
2.2	OCP	heating up	70 °C 0 mA/cm²	-
2.3	Galvanodynamic	ramp up	current ramp: 5 mA/(cm²*s)	120
2.4	Galvoanostatic	constant current	600 mA/cm²	-
3	OCP	end	0	20

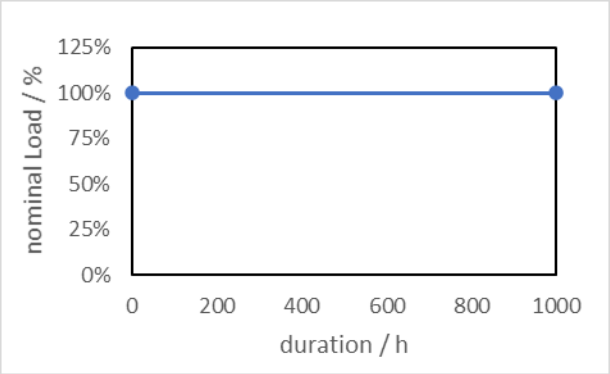

3.2 Dynamic load profiles

Dynamic load refers to the application of fluctuating current profiles instead of constant current operation. This approach simulates the non-stationary power supply characteristic of renewable energy sources and may therefore act as a relevant stressor for electrodes in alkaline electrolysis.

In the document "*EU Harmonised Protocols for Testing of Low-Temperature Water Electrolysers*" (Tsotridis and Pilenga 2021, JRC 122565) the JRC defines two AST profiles addressing dynamic load operation: the reactivity profile (JRC 122565, Section 7.7.4) and the flexibility profile (JRC 122565, Section 7.7.3).

These profiles were adapted in this work to represent high-frequency load variations suitable for electrode testing in single-cell configurations. These profiles are applicable for both cathodes and anodes and may also be performed in full-cell- as well as half-cell-setups.

3.2.1 Flexibility profile

The flexibility load profile simulates operating conditions in which the system and the electrodes are subjected to frequent load variations (Tsotridis and Pilenga 2021). Compared to real-world operation, the profile applies increased test severity by employing highly frequent load changes and elevated current ramp rates, thereby accelerating degradation effects.

The flexibility profile (see Table 4) consists of 411 repeating loops in which the load is increased stepwise every 60 s from 25 % to 100 % of the nominal load, corresponding in this work to 600

Clean Hydrogen Partnership Co-funded by the European Union
The project is supported by the Clean Hydrogen Partnership and its members

mA cm^{-2}, with increments of 25 % per step. After reaching and holding 100 % of the nominal load, the current is reduced again in 25 % steps down to 25 % of the nominal load, after which the loop is repeated.

Table 4: detailed description of the flexibility profile

Temperature [°C]	KOH concentration [wt. %]	Electrolyte flow [ml/(min*cm²)]	Operation mode	Profile suitable for
70	30	natural convection	dynamic	Anode & Cathode
Step	**Sequence**	**Function**	**parameters**	**Duration [s]**
1	OCP	start	0 mA/cm²	20
Loop start x411				
2	Galvanostatic	constant current	25 % Load (150 mA/cm²)	60
3	Galvanostatic	constant current	50 % Load (300 mA/cm²)	60
4	Galvanostatic	constant current	75 % Load (450 mA/cm²)	60
5	Galvanostatic	constant current	100 % Load (600 mA/cm²)	60
6	Galvanostatic	constant current	75 % Load (450 mA/cm²)	60
7	Galvanostatic	constant current	50 % Load (300 mA/cm²)	60
8	Galvanostatic	constant current	25 % Load (150 mA/cm²)	60
Loop end				
9	OCP	end	0 mA/cm²	20

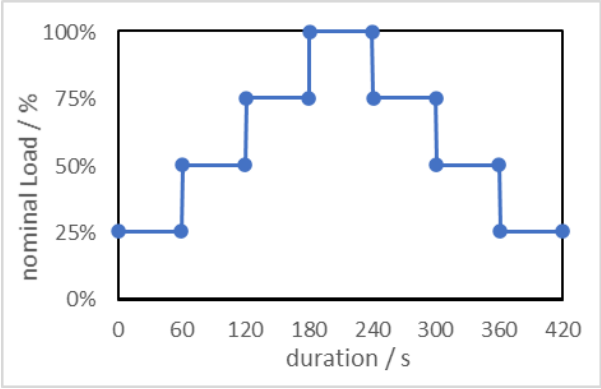

Alternatively, each load step can be held for 900 s, corresponding to the original JRC 122565 flexibility profile. While this approach still represents increased test severity compared to real-world operation, it results in a lower number of load changes than the profile proposed in this work and summarised in Table 4.

3.2.2 Reactivity profile

The reactivity profile (see Table 5) simulates grid-balancing events in which the electrolyser must rapidly ramp its load up and down to compensate for over- or under-supply in the electricity grid. The profile applied in this work follows the JRC approach (Tsotridis and Pilenga 2021). It consists of a repetitive load sequence in which the current is alternately reduced from and stepped back to the nominal load. Starting from 100 % of the nominal load, the current is reduced to 75 % and subsequently increased back to 100 %. This sequence is then repeated

Clean Hydrogen Partnership Co-funded by the European Union The project is supported by the Clean Hydrogen Partnership and its members

for 50 %, 25 %, and 0 % of the nominal load. After reaching 0 %, the load is increased again in reverse order, i.e. from 0 % to 25 %, 50 %, 75 %, and finally back to 100 % of the nominal load. Each load level is held for 60 s before the next current increase or decrease. The complete sequence constitutes one loop of the reactivity profile and is repeated 192 times, resulting in a total test duration of 48 hours.

Table 5: detailed description of reactivity profile

Temperature [°C]	**KOH concentration** [wt. %]	**Electrolyte flow** [ml/(min*cm²)]	**Operation mode**	**Profile suitable for**
70	30	natural convection	dynamic	Anode & Cathode
Step	**Sequence**	**Function**	**parameters**	**Duration [s]**
1	OCP	start	parameters	20
Loop start x192				
2	Galvanostatic	constant current	100 % Load (600 mA/cm²)	60
3	Galvanostatic	constant current	75 % Load (450 mA/cm²)	60
4	Galvanostatic	constant current	100 % Load (600 mA/cm²)	60
5	Galvanostatic	constant current	50 % Load (300 mA/cm²)	60
6	Galvanostatic	constant current	100 % Load (600 mA/cm²)	60
7	Galvanostatic	constant current	25 % Load (150 mA/cm²)	60
8	Galvanostatic	constant current	100 % Load (600 mA/cm²)	60
9	Galvanostatic	constant current	0 % Load	60
10	Galvanostatic	constant current	100 % Load (600 mA/cm²)	60
11	Galvanostatic	constant current	25 % Load (150 mA/cm²)	60
12	Galvanostatic	constant current	100 % Load (600 mA/cm²)	60
13	Galvanostatic	constant current	50 % Load (300 mA/cm²)	60
14	Galvanostatic	constant current	100 % Load (600 mA/cm²)	60
15	Galvanostatic	constant current	75 % Load (450 mA/cm²)	60
16	Galvanostatic	constant current	100 % Load (600 mA/cm²)	60
Loop end				
17	OCP	end	0 mA/cm²	20

Clean Hydrogen Partnership Co-funded by the European Union
The project is supported by the Clean Hydrogen Partnership and its members

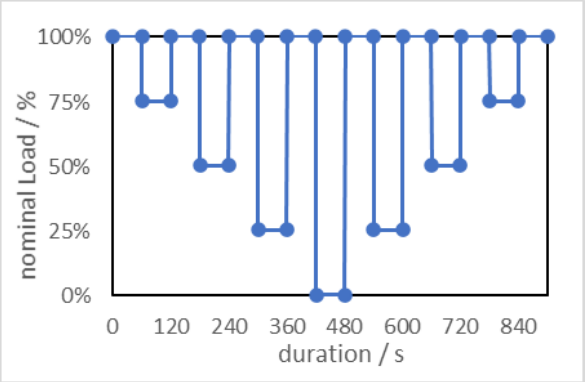

3.3 Excessive load profile

Excessive load profiles describe operating conditions in which current densities applied to the electrodes exceed the nominal load specified by the manufacturer. In large-scale electrolysers with cell areas exceeding 1 m², the current distribution across the electrode surface is often non-uniform. As a result, certain regions of the electrode may experience significantly higher local current densities than the nominal value, while other regions operate at lower current densities. Such inhomogeneities can arise, for example, from partial blockage of the electrode surface by gas bubbles. These bubbles increase local ohmic resistance, thereby reducing the local current density in affected areas, while neighbouring, unblocked regions are subjected to elevated current densities. In addition, non-uniform current supply from the bipolar plate can further contribute to spatial variations in current distribution. Beyond these intrinsic effects, electrolysers are sometimes deliberately operated under overload conditions—typically between 110 % and up to 150 % of the nominal load—for short periods, for example to stabilise electricity grids during excess power generation (e.g. commercial systems such as the 5 MW Starbase stack by OÜ Stargate Hydrogen Solutions).

Motivated by these real-world operating conditions, three constant-load ASTs are proposed to investigate high-current operation. These tests simulate current densities corresponding to approximately 170 % (1 A cm^{-2}), 330 % (2 A cm^{-2}), and 500 % (3 A cm^{-2}) of the nominal load used in this work. Each AST is conducted as a constant-load experiment with the applied current density maintained for a total duration of 48 hours. The protocols are shown in the following Table 6.

Clean Hydrogen Partnership Co-funded by the European Union
The project is supported by the Clean Hydrogen Partnership and its members

Table 6: detailed description of high current profiles with a) 170 % load, b) 330 % load and c) 500 % load

Temperature [°C]	KOH concentration [wt. %]	Electrolyte flow [ml/(min*cm²)]	Operation mode	Profile suitable for
70	30	natural convection	steady	Anode & Cathode
Step	**Sequence**	**Function**	**Parameters**	**Duration [s]**
a) 1	OCP	start	0	20
a) 2	Galvanostatic	constant current	~170 % Load 1 A/cm²	172800
a) 3	OCP	end	0	20
b) 1	OCP	start	0	20
b) 2	Galvanostatic	constant current	~330 % Load 2 A/cm²	172800
b) 3	OCP	end	0	20
c) 1	OCP	start	0	20
c) 2	Galvanostatic	constant current	~500 % Load 3 A/cm²	172800
c) 3	OCP	end	0	20

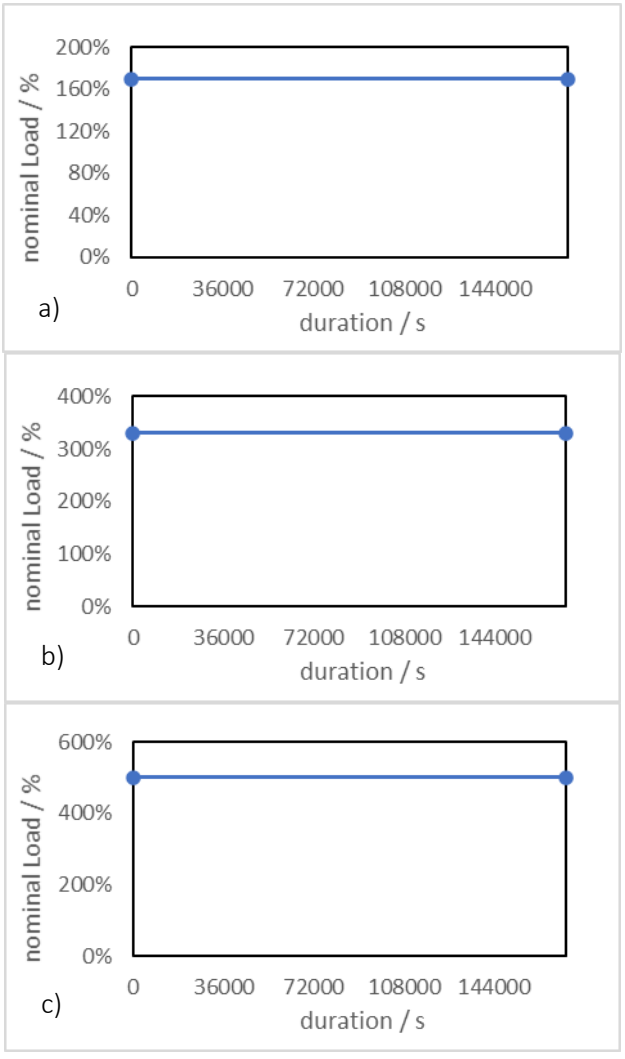

Clean Hydrogen Partnership Co-funded by the European Union
The project is supported by the Clean Hydrogen Partnership and its members

For many newly developed electrodes with a low technology readiness level, the nominal current density at which stable operation over the electrode lifetime can be ensured without accelerated damage is often unknown. The ASTs proposed herein can therefore be used to identify the current density thresholds beyond which the electrode exhibits increased damage and degradation.

It should also be noted that the current density target for 2030 set by the Clean Hydrogen Undertaking is 1 A cm^{-2} (Clean Hydrogen Joint Undertaking), a value that is already achieved by advanced state-of-the-art electrodes, such as those developed within Work Package 2 of the ENDURE project. As the proposed protocol is defined relative to the nominal load, the profiles remain applicable to future applications in which nominal current densities exceed the value of 600 mA cm^{-2} used in this work. These profiles are valid for both cathodes and anodes and may also be performed in full-cell setups.

The European partner project “Electrolife” also proposes high-current profiles as accelerated stress tests (ASTs), where “high current” is defined as 200% of the nominal current, which in their case equals 2 A cm^{-2}. In contrast to the present work, they recommend a combination of dynamic cycling and high-current operation. Their high-current AST consists of two-step cycles, maintaining a current of 200% of the nominal value for 30 seconds and then reducing it to 20% of the nominal current for 30 seconds (Briguglio and Aricò 2024).

3.4 On-Off-cycling profile

Repetitive on–off cycles represent electrolyser shutdown events, which may occur intentionally, for example during grid balancing operations, or unintentionally as a result of emergency shutdowns. In case of an electrolyser being directly connected to a solar energy source between 365 and 500 on-off cycles per year are expected (Briguglio and Aricò 2024). In this part regarding on-off cycling, shutdown events are considered under conditions where the electrodes—particularly the cathodes—are protected against reverse currents and therefore do not undergo a change in polarisation. Reverse currents themselves are explicitly addressed in Chapter 3.5. In practical systems, reverse cell currents during shutdown can be avoided by applying a low protective current or voltage, by intelligent cell design in which the anode and cathode material combination suppresses reverse currents, by unipolar electrolyser designs allowing individual cells to be switched to open circuit, or by dedicated cathodic protection systems (Kim et al. 2022).

The stressor investigated in this AST is the repetitive immediate step-up and step-down of current, resulting in cyclic transitions between high gas bubble evolution during operation and relaxation phases with negligible bubble production. The profile consists of 288 repeated loops in which the electrode is operated at 100 % nominal load (600 mA cm^{-2}) for 300 s, followed by a simulated shutdown phase operated at a protective current of 50 mA cm^{-2} for 300 s. This results in a total AST duration of approximately 48 h. The protective current was selected to ensure stable operation with industrial rectifiers while avoiding excessive current ripple that could introduce additional electrode stress. If reverse currents can be reliably excluded, the protective current may be reduced below 50 mA cm^{-2}, down to 0 mA cm^{-2} (open-circuit conditions). In the experimental campaign, both 50 mA cm^{-2} (On/-50 mA/cm^2) and 0 mA cm^{-2} (On/OCP) were applied during the shutdown phase, with no measurable difference in electrode performance. Based on these results, it is concluded that protective currents below 50 mA cm^{-2} do not significantly change the electrode behaviour under the conditions investigated. The profile is valid for both cathode and anode and may also be performed in full-cell setups. Table 7 describes the protocol for this AST.

Clean Hydrogen Partnership Co-funded by the European Union The project is supported by the Clean Hydrogen Partnership and its members

Table 7: detailed description of repetitive on-off cycles with instant load changes

Temperature [°C]	KOH concentration [wt. %]	Electrolyte flow [ml/(min*cm²)]	Operation mode	Profile suitable for
70	30	natural convection	dynamic	Anode & Cathode
Step	**Sequence**	**Function**	**parameters**	**Duration [s]**
1	OCP	start	0 mA/cm²	20
Loop start x288				
2	Galvanostatic	constant current	100 % Load (600 mA/cm²)	300
3	Galvanostatic	constant current	protective currents (50 mA/cm²)	300
		Loop end		
4	OCP	end	0 mA/cm²	20

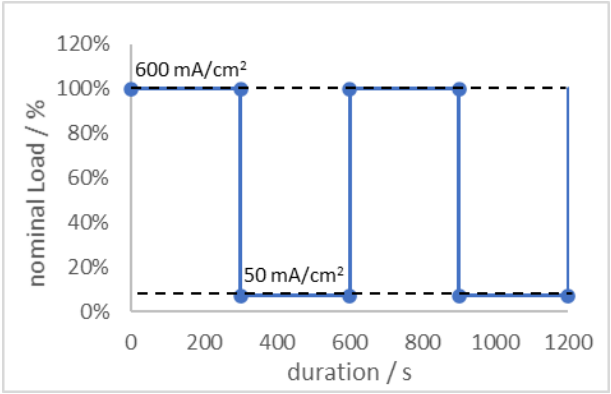

In addition to the repetitive on–off protocol presented above, we propose a less stressful AST in which the current is ramped smoothly between the nominal load of 100 % (600 mA cm^{-2}) and the protective current (50 mA cm^{-2}) at a rate of 5 mA cm^{-2} s^{-1}, rather than switched instantaneously. This approach eliminates the stress of abrupt load changes, which can occur in real shutdown situations, while still capturing the effects of full-load operation with high gas bubble evolution and subsequent relaxation. In this modified protocol, the load phase lasts 300 s, consisting of a ramp-up of 120 s, a constant full-load period of 60 s at 100 %, and a ramp-down of 120 s. The shutdown phase at the protective current also lasts 300 s. Each combination of load phase and shutdown phase forms one loop of 600 s, which is repeated 288 times, resulting in a total AST duration of approximately 48 h. Table 8 summarises the modified protocol.

Clean Hydrogen Partnership Co-funded by the European Union
The project is supported by the Clean Hydrogen Partnership and its members

Table 8: detailed description of repetitive on-off cycles with smooth load changes

Temperature [°C]	KOH concentration [wt. %]	Electrolyte flow [ml/(min*cm²)]	Operation mode	Profile suitable for
70	30	natural convection	dynamic	Anode & Cathode
Step	**Sequence**	**Function**	**parameters**	**Duration [s]**
1	OCP	start	0 mA/cm²	20
Loop start x288				
2	Galvanodynamic	ramp up	50 - 600 mA/cm² ramp: 5 mA/(cm²*s)	120
3	Galvanostatic	constant current	100 % Load (600 mA/cm²)	60
4	Galvanodynamic	ramp down	600 - 50 mA/cm² ramp: 5 mA/(cm²*s)	120
5	Galvanostatic	constant current	protective currents (50 mA/cm²)	300
		Loop end		
6	OCP	end	0 mA/cm²	20

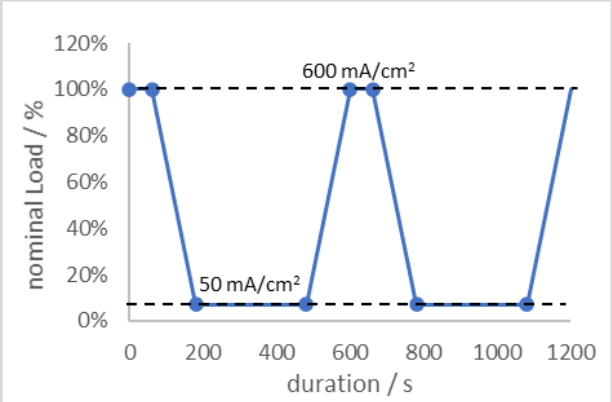

Note that the on–off cycle protocol with smooth load changes (see Table 8) has not been experimentally tested in this project and is proposed as a potential approach to reduce the stressfulness of the original on–off cycling protocol.

Marquez et al. (2024) proposes a similar approach as a stability test with on-off cycling for single cell setups which alternates between low load of 60 mA cm^{-2} for 10 minutes and high loads of 480 mA cm^{-2} for 20 minutes repeated 120 times for a total duration of 60 hours (Marquez et al. 2024). Briguglio et al. (2024) suggests a profile similar to that presented in Table 7, consisting of an on-step at 120% of the nominal current density for 120 s, followed by an off phase at either open-circuit potential (OCP) or at 15 % of the nominal current for 120 s (Briguglio and Aricò 2024).

3.5 Reverse currents profile

Reverse currents occur when a bipolar electrolyser with a serial connection of cells is shut down and the anode and cathode on each side of the bipolar plate equalize their potentials. Bipolar electrolyser configurations with serial electrical connection are the most common design for alkaline electrolysers; therefore, if no explicit measures are implemented to avoid

Clean Hydrogen Partnership Co-funded by the European Union
The project is supported by the Clean Hydrogen Partnership and its members

reverse currents, they will occur during shutdown when no external current or voltage is applied to the stack.

The potential reached by anode and cathode after shutdown depends on the oxidation state of both electrodes and is therefore strongly influenced by electrode type and material composition. Most likely, the cathode and anode potentials end up in an anodic potential region between approximately +0.2 and +1.2 V versus RHE, as shown in the experiments of Abdel Haleem et al. (2022). They further demonstrated that combining different anode types with a given cathode type leads to significantly different final potentials after shutdown. Reverse currents after shutdown depend on the cathode and anode material, cell temperature, and electrolyte flow conditions, whereas the nominal operating current density has only a minor influence (Abdel Haleem et al. 2022). We additionally expect the cell area, cell design, and prior operating duration to affect the reverse currents.

The cathode is strongly affected by reverse currents because it is transferred from a reductive into an oxidative state, which may lead to electrode degradation. In the ENDURE project, we focus on nickel-based cathodes, which are also the predominant choice in current industrial alkaline electrolysers and are expected to remain the standard for future installations (Zhang et al. 2023). The reverse-current ASTs proposed here are therefore designed specifically for nickel-based cathodes. When a nickel cathode is driven into an oxidative state by reverse currents, the density of the metallic lattice decreases and the lattice expands (Medway et al. 2006), inducing mechanical stress in the electrode structure. Repetitive oxidation–reduction cycling can therefore cause severe structural degradation of nickel electrodes.

Since different anodic potentials lead to different oxidation states and therefore to different degradation mechanisms, we define three characteristic anodic potential regions for the cathode. These regions are derived from the work of Hall et al. (2013), who proposed electrode processes of nickel electrodes at different anodic potentials. Around +0.4 V, metallic nickel oxidizes to NiO_x and $\alpha - Ni(OH)_2$ and absorbed hydrogen is oxidized and released into the electrolyte. Around +0.7 V, the $NiO_x/\ \alpha - Ni(OH)_2$ layer is chemically modified and thickens. Around +1.1 V, $\beta - Ni(OH)_2$ forms electrochemically (Hall et al. 2013). Because the anodic potential of the cathode after shutdown is usually not exactly known, we propose to test these three characteristic potential regions in separate AST protocols.

Within the ENDURE project we analysed cell behaviour in several stack tests at ZSW, including the ENDURE stack test of Work Package 4 with a cell area of 100 cm². We observed that, after shutdown, the cell voltage decreases at approximately 2 mV/s during the first 1000 s; this period corresponds to the main reverse-current activity. 90 minutes after shutdown, the voltage change is < 1 mV/min, and after 180 minutes it is < 0.3 mV/min. In these evaluations, only the cell voltage could be monitored; individual electrode potentials and reverse currents could not be measured directly. Similar behaviour was reported by Abdel Haleem et al. (2022), who used a four-cell serial test setup that allowed direct measurement of reverse currents and electrode overpotentials versus RHE. They showed that the potential change remains below 2 mV/s after shutdown and that ionic reverse currents largely disappear after approximately 5000 s (Abdel Haleem et al. 2022).

Based on these observations, we propose the following profiles to evaluate cathodes under the influence of reverse currents. These profiles are designed exclusively for cathodes and must be carried out in a half-cell setup because measurement of the cathode overpotential is essential.

Clean Hydrogen Partnership Co-funded by the European Union The project is supported by the Clean Hydrogen Partnership and its members

The AST consists of recurring loops. First, the current is ramped from 0 to 600 mA cm^{-2} at 5 mA cm^{-2} s^{-1} to bring the electrode smoothly to nominal operating conditions. The nominal current density of 600 mA cm^{-2} is held for 60 s, followed by a ramp-down to 0 mA cm^{-2} at the same rate. After current interruption, an open-circuit period of 20 s is applied to prevent immediate reverse currents. As reported by Abdel Haleem et al. (2022), residual gas bubbles after shutdown increase ohmic resistance and suppress reverse currents in the first seconds.

Subsequently, reverse currents are induced by driving the cathode overpotential toward the target oxidative potential (+0.4, +0.7, or +1.1 V) at a sweep rate of 2 mV/s using linear sweep voltammetry from the open-circuit potential to the target potential. The sweep duration depends on the initial open-circuit potential and is approximately 200 s for +0.4 V, ~350 s for +0.7 V, and ~550 s for +1.1 V. After reaching the target potential, one loop is completed, and the next loop begins with a new ramp-up to nominal current density. We propose 200 loops, resulting in total test durations of ~29 h (+0.4 V), ~37 h (+0.7 V), and ~48 h (+1.1 V). Table 9 summarizes the AST profile for +0.4 V; detailed descriptions for +0.7 V and +1.1 V are provided in Appendix 9.1. The accompanying diagram illustrates the procedure: the blue curve represents the nominal load (left axis) while the orange curve shows the cathode overpotential (right axis), whereby an overpotential of −100 mV during nominal load is assumed but may vary with the cathode material.

Table 9: detailed description of reverse current profile; blue graph = nominal load, orange graph = overpotential

Temperature [°C]	**KOH concentration** [wt. %]	**Electrolyte flow** [ml/(min*cm²)]	**Operation mode**	**Profile suitable for**
70	30	natural convection	dynamic	Cathode
Step	**Sequence**	**Function**	**parameters**	**Duration [s]**
1	OCP	start	0 mA/cm²	20
Loop start x200				
2	Galvanodynamic	ramp up	0 - 600 mA/cm² ramp: 5 mA/(cm²*s)	120
3	Galvanostatic	constant current	100 % Load (600 mA/cm²)	60
4	Galvanodynamic	ramp down	600 - 50 mA/cm² ramp: 5 mA/(cm²*s)	120
5	OCP	shut down	0 mA/cm²	20
5	Linear sweep volatametry	anodic potential with reverse currents	Umin = OCP Umax = 400mV Scan rate 2mV/s	200
Loop end				
6	OCP	end	0 mA/cm²	20

Clean Hydrogen Partnership Co-funded by the European Union
The project is supported by the Clean Hydrogen Partnership and its members

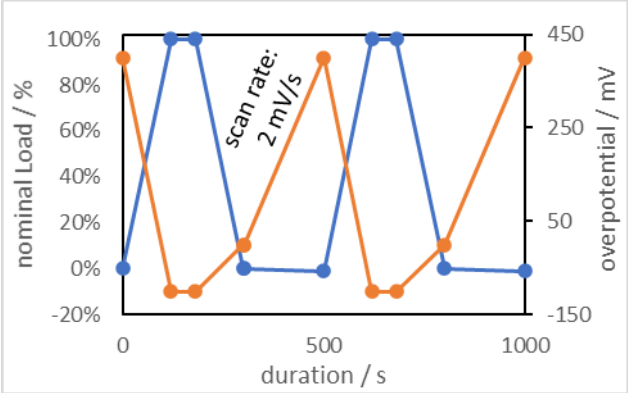

Experimental studies explicitly addressing reverse currents in alkaline electrolysis are scarce. Only a limited number of publications report stability tests of electrodes (anode and cathode) under reverse-current conditions currents (Marquez et al. 2024; Abdel Haleem et al. 2021; Han et al. 2020; Kim et al. 2023). The central challenge in designing ASTs for reverse currents is reproducing shutdown behaviour that is representative of real electrolyser operation. It is not sufficient to simply apply a reverse current or reverse potential; if the reverse-current profile is not realistic, electrodes may be subjected to unrealistically harsh conditions and be excessively damaged.

In our approach, we attempt to reproduce realistic reverse-current behaviour based on stack data from ENDURE tests as well as on the comprehensive study of Abdel Haleem et al. (2022). However, given the still limited understanding of the actual shutdown processes in alkaline electrolysers, we do not claim that the half-cell ASTs described above perfectly replicate real operating conditions. We emphasize the need for further research into reverse-current phenomena and for continued development of AST protocols addressing such effects. Nevertheless, the ASTs proposed here provide clear indications of whether cathodes are tolerant to reverse currents or whether reverse-current exposure constitutes a strongly damaging process.

Since the reverse-current ASTs in this work focus exclusively on cathodes, it should be noted that Abdel Haleem et al. (2021) proposed a similar AST protocol for anodes. In their approach, the anode was first operated at 600 mA cm^{-2} for 60 s, followed by linear sweep voltammetry from the open-circuit potential (approximately 1.5 V) to +0.3, +0.5, or +0.7 V at sweep rates of 50 or 500 mV s^{-1}. The potential was subsequently held at the final value for 10–60 s. This loop was repeated 2000 times, resulting in a total test duration of approximately 70 h.

3.6 Impurity profile

Impurities in the electrolyte may lead to deposits on the cathode or anode during electrolysis or during shutdown of the electrolyser. The effects of specific foreign elements in the electrolyte may differ significantly between anode and cathode. Such impurities can either deteriorate or improve electrode performance. Becker et al. summarize the effects described in literature of selected elements in the lye on cathodes and anodes in alkaline electrolysis (Becker et al. 2023). Investigating the influence of individual elements in the electrolyte on electrode behaviour represents an extensive research field that could not be fully covered within the present project. Our approach is to analyse the degradation of cathodes under the influence of industrial electrolyte as it is composed after electrolysis. Almost all industrial electrolysers consist of peripheral components made of stainless steel. Elements contained in the stainless steel can dissolve into the electrolyte and thus form impurities. For this AST, we

Clean Hydrogen Partnership Co-funded by the European Union
The project is supported by the Clean Hydrogen Partnership and its members

therefore used electrolyte that had been operated in an alkaline electrolyser test system at ZSW for approximately 400 hours. This electrolyte was analysed by ICP-OES to quantify the mass fractions of the impurities; the results are presented in Table 10. In this AST profile, the effect of impure electrolyte is evaluated by exposing the tested electrode to the contaminated electrolyte during one of the AST profiles described above, instead of using high-purity KOH, which is the standard for laboratory single-cell tests (Appelhaus et al. 2024). We propose the following profiles for the impurity AST series:

- Reference profile (see Table 2)
- Flexibility profile (see Table 4)
- On–off cycling (see Table 7)

Table 10: Measured mass fractions in the electrolyte for the impurity AST profile

Ca	Cr	Cu	Fe	Mg	Ni	Si	Zn	Al	Mo
					[mg kg^{-1}]				
0.61	34.77	0.32	4.63	0.09	0.31	23.10	8.65	24.00	37.00

3.7 Outlook on additional relevant stressors

The following list outlines and explains stressors that may be relevant for AEL electrodes but were not addressed in the experimental scope of this work and therefore were not assigned dedicated test protocols. These stressors may serve as a basis for extending and further developing the AST protocols presented in this study.

- High lye/water inlet flow rate: High lye/water inlet flow rates could accelerate catalyst loss due to dissolution/erosion effects (Malkow and Pilenga 2024)
- Low lye/water inlet flow rate: Too low lye/water inlet flow rates may result in insufficient wetting, risking dry active area and a reduction in gas bubble removal which could result in hotspots and overpotential increases (Malkow and Pilenga 2024)
- Lye temperature variation: Variations in the lye temperature cause corresponding changes in the overall cell temperature. These temperature fluctuations induce mechanical stress in the cell components, including the electrodes, due to thermal expansion and contraction. Such stresses can accelerate the degradation of both the electrodes and their catalysts.
- High operating temperature (> 80 °C) and low operating temperature (< 60 °C): The cell temperature affects the temperature-dependent reaction kinetics of the electrodes (Malkow and Pilenga 2024). Additionally, material changes may occur, although these are unlikely at the temperature windows typical for alkaline electrolysis (20 °C – 90 °C).
- Differential pressure between anode and cathode: A pressure difference between the anode and cathode half-cells exerts mechanical stress on the electrode in the lower-pressure half-cell. This stress is primarily transmitted through the diaphragm, especially in zero-gap configurations, and can contribute to electrode degradation.
- Pressure variation / Sudden pressure drop: Sudden pressure changes alter the density and distribution of hydrogen and oxygen bubbles. Because these bubbles are located on the electrode surfaces and within the pores of the catalytic layer, rapid changes in bubble density impose mechanical stress on the surface structure. This can destabilize the porous catalyst layer and contribute to electrode degradation.

Clean Hydrogen Partnership Co-funded by the European Union The project is supported by the Clean Hydrogen Partnership and its members

- **High pressure operation (above atmospheric pressure):** Higher operating pressures reduce gas bubble size due to the increased gas density. For electrodes with porous catalyst structures, the resulting smaller bubbles can penetrate deeper into the pore network. This may influence mass transport, alter local reaction conditions, and impose mechanical stress within deeper pore layers of the catalyst.
- **AC ripple:** Current fluctuations originating from AC/DC conversion, for example in thyristor-based power supplies, introduce an AC ripple component into the operating current. This ripple reduces the efficiency of the electrolyser, particularly under part-load conditions (Amireh et al. 2023).

In the EU harmonised protocols for testing of low temperature water electrolysers (Tsotridis and Pilenga 2021) the following stressors were defined for testing protocols for alkaline water electrolysis: high operating temperature (> 80 °C), low operating temperature (< 60 °C), high-pressure operation, and low lye/water inlet flow rate. These stressors can be incorporated into the testing procedure described in this document by adjusting the corresponding test parameters of the described reference test (see chapter 2.2) to match the JRC stressor conditions, as outlined in the following Table 11.

Table 11: Settings of AWE stressors for AWE single cell and short stack testing. From (Tsotridis and Pilenga 2021)

	PARAMETERS	UNIT	REFERENCE Setting	Cell Temperature Stressor settings		H2 Pressure Stressor settings	Electrolyte Inlet Flowrate Stressor settings	
				Test 1	Test 2	Test 3	Test 4	Test 5
	Cell/stack temperature	°C	80	50	100	80	80	80
ANODE	Electrolyte inlet temperature	°C	80	50	100	80	80	80
ANODE	Minimum Electrolyte inlet flowrate	mL.cm^{-2}.min^{-1}	1	1	1	1	0.25	2
CATHODE	Electrolyte inlet temperature	°C	80	50	100	80	80	80
CATHODE	Minimum Electrolyte inlet flowrate	mL.cm^{-2}.min^{-1}	1	1	1	1	0.25	2
CATHODE	Hydrogen outlet pressure	kPa	500	500	500	3,000([10])	500	500

In (Briguglio and Aricò 2024) the following AST protocols for stack testing and procedures have been described: dynamic load profiles, start-up / shut down profiles, high current fluctuating profiles, pressure cycling profiles and temperature cycling profiles.

4 Standardized presentation of results

The degradation of electrodes induced by ASTs needs to be quantified in a standardized manner. Since each AST is embedded in a pre- and post-characterization (see chapter 2.1), these characterization steps provide key figures that must be evaluated. The degradation of a specific electrode under a specific AST is assessed by comparing selected values from the pre-characterization, referred to as Beginning of Life (BoL), with the corresponding values from the post-characterization, referred to as End of Life (EoL). The parameters proposed for a comprehensive assessment of the AST are as follows:

Clean Hydrogen Partnership Co-funded by the European Union
The project is supported by the Clean Hydrogen Partnership and its members

- **Tafel parameters:** The exchange current density j_0 [mA cm^{-2}] and the Tafel slope b [mV dec^{-1}] are both obtained from the Tafel plot of step 5 of the characterization protocol (see Chapter 2.1). A detailed description of the calculation and interpretation of these parameters is provided in Briguglio et al. (2024, Chapter 2.3.1.1) and (Ďurovič et al. 2021).
- **Capacitive double-layer capacitance (CDL) [mF cm^{-2}]:** determined from cyclic voltammetry in step 7 of the characterization protocol (see Chapter 2.1).
- **Overpotential at defined current densities ($U(i)$):** the overpotential at 300, 600, and 1000 mA cm^{-2}, expressed in mV, obtained from the polarization curve of step 5 of the characterization protocol (see Chapter 2.1). For each current density, the average value of the last 5 seconds of the galvanostatic step is used.

The key metric for evaluating AST-induced degradation is the **degradation rate**, which describes the rate of change of the parameters listed above over the duration of the AST. In general terms, it is calculated as

$$\text{Degradation rate} = \frac{x_{EoL} - x_{BoL}}{t_{AST}} \left[\frac{1}{h}\right] \quad (4.1)$$

where x_{BoL} is the value at BoL, x_{EoL} the value at EoL, and t_{AST} is the total AST duration.

The primary indicator used to quantify the effect of the AST is the potential degradation rate $\dot{U}_{AST}(i)$ at a given current density i . It is defined as the difference between the BoL potential $U_{BoL}(i)$ and the EoL potential $U_{EoL}(i)$, divided by the total AST duration t_{AST} and is presented in [µV/h]:

$$\dot{U}_{AST}(i) = \frac{U_{EoL}(i) - U_{BoL}(i)}{t_{AST}} \left[\frac{\mu V}{h}\right] \quad (4.2)$$

It is important to note that the interpretation of the sign (positive or negative) of the degradation rate depends on the electrode type (cathode or anode) in half-cell measurements. For cathode investigations, a negative degradation rate indicates a loss of performance, whereas for anode investigations a positive degradation rate corresponds to performance loss, i.e., deterioration induced by operation under the AST conditions in the half-cell setup. For full-cell measurements a positive degradation rate consistently indicates performance loss.

5 Experimental results

The ASTs described above were validated within Task 4.1 at ZSW. Therefore, Raney nickel cathodes on perforated sheet substrates (Rv 1.5–2.5) were used, which represent a pre-development of Task 2.6, “Increasing the surface area of PTE via zinc coating processes.” These electrodes were further characterized using the harmonized half-cell testing protocol described in D1.2 (Martínez et al. 2024).

Without the application of any AST, the cathodes used in this study showed an average overpotential of −226 mV vs. RHE at a current density of 1000 mA cm^{-2} (dwell time 5 h), with a standard deviation of ±6.8 mV. The average double-layer capacitance (CDL) was 182.6 mF cm^{-2}, with a standard deviation of ±17.8 mF cm^{-2}. The exchange current density (j_0)

Clean Hydrogen Partnership Co-funded by the European Union The project is supported by the Clean Hydrogen Partnership and its members

was 0.65 mA cm^{-2}, with a standard deviation of ±0.15 mA cm^{-2}. The Tafel slope (b) was −49.37 mV dec^{-1}, with a standard deviation of ±3.4 mV dec^{-1}.

The following Figure 2 shows the overpotential versus RHE for all pre-characterization measurements of the same cathode type at 1000 mA cm^{-2}.

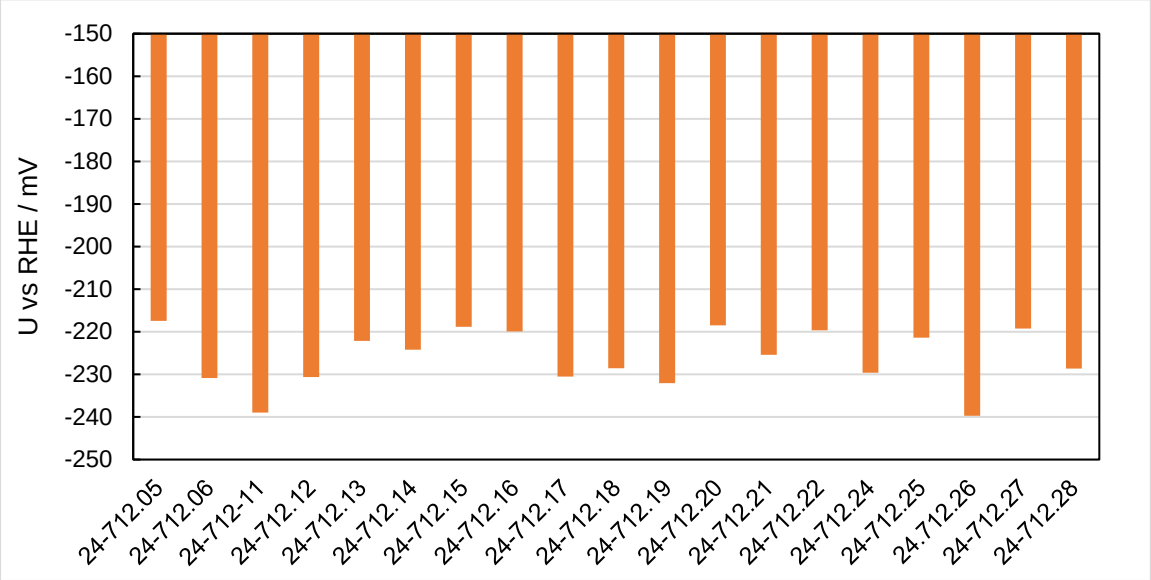

Figure 2: overpotential vs. RHE of all pre-characterization measurements at a current density of 1000 mA cm $^{-2}$, 70 °C, 30 wt. % KOH

The following Table 12 presents the experimental degradation rates of the ASTs described in Chapter 3 for the exchange current density (j_0) in µA cm^{-2} h^{-1}, the Tafel slope (b) in µV dec^{-1} h^{-1}, the capacitive double-layer capacitance (CDL) in mF cm^{-2} h^{-1}, and the cathode overpotential vs. RHE ($\dot{U}(i)$) in µV h^{-1} at 300, 600 and 1000 mA cm^{-2}. The AST protocols were tested multiple times experimentally on the cathodes described above. The table reports the results for two reference tests (Reference_1 and Reference_2); the Flexibility and Reactivity profiles from the category of dynamic load profiles; the on–off cycling protocol with the off step at OCP (On/OCP) and with the off step at a protection current of −50 mA cm^{-2} (On/-50 mA/cm²); three reverse-current profiles with reverse potentials of +0.4 V vs. RHE (Reverse +0.4 V), +0.7 V vs. RHE (Reverse +0.7 V), and +1.1 V vs. RHE (Reverse +1.1 V); excessive load profiles with high currents (HC) of 1 A cm^{-2} (HC 1 A/cm²), 2 A cm^{-2} (HC 2 A/cm²), and 3 A cm^{-2} (HC 3 A/cm²); and three impurity profiles (Imp) based on the reference profile (Imp Reference), the Flexibility profile (Imp Flexibility), and the on–off cycles profile (Imp On/-50 mA/cm²).
To facilitate interpretation of the results, the degradation based on the overpotential degradation rate is highlighted using colour coding: green indicates that the AST protocol resulted in no degradation or even a performance improvement; yellow indicates minor degradation induced by the AST; and red indicates severe degradation and damage.

Clean Hydrogen Partnership Co-funded by the European Union
The project is supported by the Clean Hydrogen Partnership and its members

Table 12: Overview of AST results

	io	b	CDL	$\dot{U}\left(300\frac{mA}{cm^2}\right)$	$\dot{U}\left(600\frac{mA}{cm^2}\right)$	$\dot{U}\left(1000\frac{mA}{cm^2}\right)$
	µA cm^{-2}h^{-1}	µV dec^{-1} h^{-1}	mF cm^{-2}h^{-1}	µV h^{-1}		
Reference						
Reference_1	5.1	30	-0.47	-20	-132	-196
Reference_2	5.3	6	-0.24	43	9	-4
Dynymic load profile						
Flexibility	-4.3	264	-0.27	-158	-105	-302
Reactivity	4.4	38		92	-15	-35
On- Off-cycles						
On/OCP	3.2	-60	-0.66	17	-65	-74
On/-50 mA/cm²	-7.0	260	-0.13	-13	58	-26
Reverse currents						
Reverse + 0.4 V				-6136	-6935	-6731
Reverse + 0.7 V	-10.5	-221	-4.71	-4890	-5157	-5309
Reverse + 1.1 V	-2.1	19	-3.08	-2744	-2768	-2772
Exessive load profiles						
HC 2 A/cm²	0.8	34	-0.63	-128	-226	-248
HC 3 A/cm²	0.7	-19	-1.26	-490	-587	-578
HC 1 A/cm²	1.2	33	-0.40	4	49	138
Impurities						
Imp Reference	-2	224	-0.55	1008	1171	1236
Imp Flexibility	-3	232	-0.03	1233	1557	1632
Imp On/-50 mA/cm²	-1	137	0.39	1169	1926	1434

As one of the two test repetitions of the reference profile (compare chapter 2.2) already shows slight degradation, experiencing an overpotential increase of |132 µV h^{-1}| at 600 mA/cm² over the 48 h constant-load profile, it becomes evident that a moderate performance decrease, as observed for Reference_1, must not necessarily be a direct effect of the AST but lies within the range of natural degradation induced by constant load. The results therefore show that the protocols based on dynamic load profiles (compare chapter 3.2) and On-Off-cycles (compare chapter 3.4) do not impose degradation beyond that of the constant-load reference profile for the cathodes investigated in this study.

The AST based on electrolyte impurities where the impure lye originates from a former AEL stack test run (compare chapter 3.6) induces a significant performance improvement compared to cathodes investigated under high-purity electrolyte. This performance increase for the cathodes of this study is attributed primarily to the presence of iron and possibly chromium in the AST electrolyte. Literature reports that iron may increase cathodic performance (Mauer et al. 2007; Flis-Kabulska and Flis 2014; Becker et al. 2023).

The excessive load profiles show particularly interesting results. Under constant current application at 1 A cm^{-2} (HC 1 A/cm²), the cathode does not suffer degradation but instead shows a slight improvement in performance. This indicates that the investigated cathode type can withstand constant loads at 1 A cm^{-2}, similarly to the nominal current density of 600 mA cm^{-2} defined in this study, at least over moderate time periods. When the current is increased to 2 A cm^{-2} (HC 2 A/cm²), enhanced performance loss becomes evident compared to the reference profiles, indicating that this cathode type should not be operated at 2 A cm^{-2} or higher. At 3 A cm^{-2} (HC 3 A/cm²), the cathode experiences severe degradation, with the

Clean Hydrogen Partnership Co-funded by the European Union The project is supported by the Clean Hydrogen Partnership and its members

degradation rate being more than twice as high as that of the reference profile. For HC 2 A/cm² and especially HC 3 A/cm², the degradation rate of the CDL is significantly higher than for the reference profile. This indicates an increased loss of catalytically active surface area when excessive loads are applied to this cathode type. This was also supported by SEM observations, where the cathode (HC 3 A/cm²) showed multiple cracks and damage on the Raney nickel surface.

The observed decrease in CDL is consistently present for this cathode type across all investigated ASTs. It remains to be determined whether this trend reflects a continuous degradation mechanism or a transient stabilization process of the electrode surface. This question will be addressed by evaluating the long-term constant-load profile. An alternative explanation is that the cathode had not yet reached a steady state when the AST and reference profiles commenced, such that residual conditioning effects were still present during the respective profiles. The long-term constant-load profile is currently ongoing and has therefore not been included in the present evaluation. For the profiles Reverse + 0.4 V and Reactivity, experimental inconsistencies, caused by the potentiostat, occurred during the post-characterisation measurements, resulting in missing values for the Tafel parameters and the CDL.

The complete results of the experimental part of this deliverable can be found in Appendix 1.1

6 Deviations

Originally, the cell temperature for the single-cell ASTs was set to 80 °C, as specified in D1.2, *"Report on Harmonised Test Protocols Adopted for ENDURE."* At this temperature, the evaporation rate of water and KOH within the cell setup was high, resulting in noticeable changes in electrolyte concentration. As a stable electrolyte concentration is essential for reproducible AST results, the operating temperature was reduced to 70 °C. This adjustment significantly lowered the evaporation rate and ensured a stable electrolyte concentration over the entire test duration.

The present deliverable report was finalized after the official due date (December 2025). The delayed submission of the written report had no impact on the project progress, results, or subsequent activities.

7 Conclusions

This report presents a comprehensive methodology for assessing electrode degradation in alkaline electrolysis through the application of accelerated stress tests (ASTs) in single-cell configurations. Rather than focusing on a single degradation mechanism, as is common in the limited literature on ASTs to date, this work addresses a broad spectrum of stressors relevant to real-world operation. It consolidates them into five AST profile series targeting distinct degradation phenomena and comparing those with a defined reference profile. The protocols are described in detail to enable reproducibility and further development by other research groups. Experimental investigations on Raney nickel cathodes demonstrate that excessive load and reverse-current operation impose particularly severe stress, whereas dynamic loading and on–off cycling do not generate comparably pronounced degradation. Notably, impurities originating from stainless-steel components of industrial electrolysis systems were found to enhance cathode performance. Ongoing collaboration within the project consortium and the JRC, together with future experimental results, will support iterative optimization of the

Clean Hydrogen Partnership Co-funded by the European Union The project is supported by the Clean Hydrogen Partnership and its members

proposed protocols and their practical relevance. The protocols developed here will also be applied to electrodes produced within Work Package 2, thereby expanding the experimental foundation on which the methodology is built.

Clean Hydrogen Partnership
Co-funded by the European Union
The project is supported by the Clean Hydrogen Partnership and its members

8 List of References

Abdel Haleem, Ashraf; Huyan, Jinlei; Nagasawa, Kensaku; Kuroda, Yoshiyuki; Nishiki, Yoshinori; Kato, Akihiro et al. (2022): Effects of operation and shutdown parameters and electrode materials on the reverse current phenomenon in alkaline water analyzers. In *Journal of Power Sources* 535, p. 231454. DOI: 10.1016/j.jpowsour.2022.231454.

Abdel Haleem, Ashraf; Nagasawa, Kensaku; Kuroda, Yoshiyuki; Nishiki, Yoshinori; ZAENAL, Awaludin; Mitsushima, Shigenori (2021): A New Accelerated Durability Test Protocol for Water Oxidation Electrocatalysts of Renewable Energy Powered Alkaline Water Electrolyzers. In *Electrochemistry* (2), pp. 186–191. DOI: 10.5796/electrochemistry.20-00156.

Amireh, Senan F.; Heineman, Niels N.; Vermeulen, Paul; Barros, Rodrigo Lira Garcia; Yang, Dongsheng; van der Schaaf, John; Groot, Matheus T. de (2023): Impact of power supply fluctuation and part load operation on the efficiency of alkaline water electrolysis. In *Journal of Power Sources* 560, p. 232629. DOI: 10.1016/j.jpowsour.2023.232629.

Appelhaus, Simon; Ritz, Lukas; Pape, Sharon-Virginia; Lohmann-Richters, Felix; Kraglund, Mikkel Rykaer; Jensen, Jens Oluf et al. (2024): Benchmarking performance: A round-robin testing for liquid alkaline electrolysis. In *International Journal of Hydrogen Energy* 95, pp. 1004–1010. DOI: 10.1016/j.ijhydene.2024.11.288.

Becker, Hans; Murawski, James; Shinde, Dipak V.; Stephens, Ifan E. L.; Hinds, Gareth; Smith, Graham (2023): Impact of impurities on water electrolysis: a review. In *Sustainable Energy Fuels* 7 (7), pp. 1565–1603. DOI: 10.1039/D2SE01517J.

Briguglio, Nicola; Aricò, Antonino S. (2024): D4.1 – Specification, terminology and Harmonised protocols for low-temperature electrolysis. Available online at https://electrolife-project.eu/deliverable-4-1/.

Clean Hydrogen Joint Undertaking (Ed.): Stategic Research and Innovation Agenda 2021-2027. Available online at https://www.clean-hydrogen.europa.eu/document/download/8a35a59b-a689-4887-a25a-6607757bbd43_en?filename=Clean%20Hydrogen%20JU%20SRIA%20-%20approved%20by%20GB%20-%20clean%20for%20publication%20%28ID%2013246486%29.pdf.

Ďurovič, Martin; Hnát, Jaromír; Bouzek, Karel (2021): Electrocatalysts for the hydrogen evolution reaction in alkaline and neutral media. A comparative review. In *Journal of Power Sources* 493, pp. 1–17. DOI: 10.1016/j.jpowsour.2021.229708.

Flis-Kabulska, I.; Flis, J. (2014): Hydrogen evolution and corrosion products on iron cathodes in hot alkaline solution. In *International Journal of Hydrogen Energy* 39 (8), pp. 3597–3605. DOI: 10.1016/j.ijhydene.2013.12.158.

Hall, David S.; Bock, Christina; MacDougall, Barry R. (2013): The Electrochemistry of Metallic Nickel: Oxides, Hydroxides, Hydrides and Alkaline Hydrogen Evolution. In *J. Electrochem. Soc.* 160 (3), F235-F243. DOI: 10.1149/2.026303jes.

Han, Jimin; KIM, JONGWON; BAE, KIKWANG; PARK, CHUSIK; JEONG, SEONGUK; JUNG, KWANGJIN et al. (2020): Intermittent Operation Induced Deactivation Mechanism for HER of

Clean Hydrogen Partnership Co-funded by the European Union The project is supported by the Clean Hydrogen Partnership and its members

Ni-Zn-Fe Electrode for Alkaline Electrolysis. In *KHNES* 31 (1), pp. 8–22. DOI: 10.7316/KHNES.2020.31.1.8.

Kim, Ji-Eun; Kim, Tae-Hyun; Park, Chu-Sik; JUNG, KWANGJIN; Yoon, Jaekyung; Lee, Ki-Bong; Kang, Kyoung-Soo (2023): Probing the (de)activation of Raney nickel–iron anodes during alkaline water electrolysis by accelerated deactivation testing. In *Electrochemistry Communications* 157, p. 107601. DOI: 10.1016/j.elecom.2023.107601.

Kim, Yoona; Jung, Sang-Mun; Kim, Kyu-Su; Kim, Hyun-Yup; Kwon, Jaesub; Lee, Jinhyeon et al. (2022): Cathodic Protection System against a Reverse-Current after Shut-Down in Zero-Gap Alkaline Water Electrolysis. In *JACS Au* 2 (11), pp. 2491–2500. DOI: 10.1021/jacsau.2c00314.

Malkow, K. T.; Pilenga, A.; Tsotridis, G. (2018): EU harmonised polarisation curve test method for low-temperature water electrolysis. Available online at https://publications.jrc.ec.europa.eu/repository/handle/JRC104045.

Malkow, Thomas; Pilenga, Alberto (2024): EU harmonised accelerated stress testing protocols for low-temperature water electrolyser. A proposal with testing guidance for assessing performance degradation in water electrolyser stacks. Europäische Kommission. Luxembourg (EUR, JRC133726). Available online at https://op.europa.eu/en/publication-detail/-/publication/89215210-2c51-11ef-a61b-01aa75ed71a1.

Marquez, Raul A.; Espinosa, Michael; Kalokowski, Emma; Son, Yoon Jun; Kawashima, Kenta; Le, Thuy Vy et al. (2024): A Guide to Electrocatalyst Stability Using Lab-Scale Alkaline Water Electrolyzers. In *ACS Energy Lett.* 9 (2), pp. 547–555. DOI: 10.1021/acsenergylett.3c02758.

Martínez, Lidia; Ludwig, Tobias; Gil, Vanesa; van Dijk, Nicolás; Bernäcker, Christian (2024): Report on harmonised test protocols adopted for ENDURE. Deliverable 1.2. ENDURE. Available online at https://06da0203-cc2b-49bd-ad5f-09bbc8269004.filesusr.com/ugd/2f8c14_96d1ddb8fe464e8f9caca4c20577941d.pdf.

Mauer, Anne E.; Kirk, Donald W.; Thorpe, Steven J. (2007): The role of iron in the prevention of nickel electrode deactivation in alkaline electrolysis. In *Electrochimica Acta* 52 (11), pp. 3505–3509. DOI: 10.1016/j.electacta.2006.10.037.

Medway, S. L.; Lucas, C. A.; Kowal, A.; Nichols, R. J.; Johnson, D. (2006): In situ studies of the oxidation of nickel electrodes in alkaline solution. In *Journal of Electroanalytical Chemistry* 587 (1), pp. 172–181. DOI: 10.1016/j.jelechem.2005.11.013.

Tsotridis, G.; Pilenga, A. (2021): EU harmonised protocols for testing of low temperature water electrolysers. Europäische Kommission. Luxembourg (EUR, JRC122565). Available online at https://op.europa.eu/en/publication-detail/-/publication/bbbeba00-ee82-11eb-a71c-01aa75ed71a1/language-en/format-PDF/source-280217337.

Zhang, Rufei; Xie, Ao; Cheng, Linting; Bai, Zhiqun; Tang, Yang; Wan, Pingyu (2023): Hydrogen production by traditional and novel alkaline water electrolysis on nickel or iron based electrocatalysts. In *Chemical communications (Cambridge, England)* 59 (53), pp. 8205–8221. DOI: 10.1039/d3cc00996c.

Clean Hydrogen Partnership Co-funded by the European Union The project is supported by the Clean Hydrogen Partnership and its members

9 Appendix

9.1 Additional profiles on reverse currents

Reverse Current Profile with an oxidation potentail of + 0.7 V

Temperature [°C]	KOH concentration [wt. %]	Electrolyte flow [ml/(min*cm²)]	operation mode	Profile suitable for
70	30	natural convection	dynamic	Cathode
Step	**Sequence**	**Function**	**parameters**	**Duration [s]**
1	OCP	start	0 mA/cm²	20
Loop start x200				
2	Galvanodynamic	ramp up	0 - 600 mA/cm² ramp: 5 mA/(cm²*s)	120
3	Gstatic	constant current	100 % Load (600 mA/cm²)	60
4	Galvanodynamic	ramp down	600 - 50 mA/cm² ramp: 5 mA/(cm²*s)	120
5	OCP	shut down	0 mA/cm²	20
5	Linear sweep volatametry	anodic potential with reverse currents	Umin = OCP Umax = 400mV Scan rate 2mV/s	350
Loop end				
6	OCP	end	0 mA/cm²	20

Reverse Current Profile with an oxidation potentail of + 1.1 V

Temperature [°C]	KOH concentration [wt. %]	Electrolyte flow [ml/(min*cm²)]	operation mode	Profile suitable for
70	30	natural convection	dynamic	Cathode
Step	**Sequence**	**Function**	**parameters**	**Duration [s]**
1	OCP	start	0 mA/cm²	20
Loop start x200				
2	Galvanodynamic	ramp up	0 - 600 mA/cm² ramp: 5 mA/(cm²*s)	120
3	Gstatic	constant current	100 % Load (600 mA/cm²)	60
4	Galvanodynamic	ramp down	600 - 50 mA/cm² ramp: 5 mA/(cm²*s)	120
5	OCP	shut down	0 mA/cm²	20
5	Linear sweep volatametry	anodic potential with reverse currents	Umin = OCP Umax = 400mV Scan rate 2mV/s	550
Loop end				
6	OCP	end	0 mA/cm²	20

Clean Hydrogen Partnership Co-funded by the European Union
The project is supported by the Clean Hydrogen Partnership and its members

9.2 Experimental results for all profiles

Reference

Reference		BoL		EoL		Degradation rate		
	Unit	Reference_1	Reference_2	Reference_1	Reference_2	Unit	Reference_1	Reference_2
io	[mA/cm2]	0.74	0.66	0.98	0.91	µA $cm^{-2}h^{-1}$	5.086	5.322
b	[mV/dec]	-54.95	-48.54	-53.56	-48.26	µV dec -1 h-1	29.570	5.954
CDL	[mF/cm2]	176.22	197.50	153.82	186.07	mF $cm^{-2}h^{-1}$	-0.474	-0.242
300 mA/cm²	[mV]	-175.68	-158.56	-176.61	-156.56	µV h^{-1}	-19.759	42.508
600 mA/cm²	[mV]	-207.72	-194.46	-213.94	-194.02		-131.604	9.194
1000 mA/cm²	[mV]	-230.86	-221.39	-240.14	-221.59		-196.245	-4.184

Dynamic load profile

Dynamic load profile		BoL		EoL		Degradation rate					
	Unit	Flexibility	Reactivity	Flexibility	Reactivity	Unit	Flexibility	Reactivity	Unit	Flexibility	Reactivity
io	[mA/cm2]	0.84	0.91	0.68	1.10	µA $cm^{-2}h^{-1}$	-4.262	4.389	µA $cm^{-2}h^{-1}$/cycle	-0.425	0.961
b	[mV/dec]	-54.95	-51.63	-44.66	-50.03	µV dec -1 h-1	263.767	38.094	µV $dec^{-1}h^{-1}$/cycle	26.321	8.340
CDL	[mF/cm2]	172.10	188.58	161.40		mF $cm^{-2}h^{-1}$	-0.274		mF $cm^{-2}h^{-1}$/cycle	-0.027	
300 mA/cm²	[mV]	-172.67	-159.41	-178.82	-155.52	µV h^{-1}	-157.531	92.493	µV/cycle	-15.720	20.249
600 mA/cm²	[mV]	-211.70	-191.59	-215.78	-192.24		-104.583	-15.435		-10.436	-3.379
1000 mA/cm²	[mV]	-230.64	-219.64	-242.41	-221.13		-301.747	-35.454		-30.110	-7.762

On/ Off Cycle

On/ Off cycle		BoL		EoL		Degradation rate					
	Unit	On/OCP	On/-50 mA/cm²	On/OCP	On/-50 mA/cm²	Unit	On/OCP	On/-50 mA/cm²	Unit	On/OCP	On/-50 mA/cm²
io	[mA/cm2]	0.50	0.72	0.65	0.41	µA $cm^{-2}h^{-1}$	3.175	-6.968	µA $cm^{-2}h^{-1}$/cycle	0.688	-1.510
b	[mV/dec]	-42.77	-52.41	-45.52	-40.58	µV dec -1 h-1	-60.330	260.068	µV $dec^{-1}h^{-1}$/cycle	-13.071	56.348
CDL	[mF/cm2]	217.29	184.38	187.21	178.40	mF $cm^{-2}h^{-1}$	-0.661	-0.131	mF $cm^{-2}h^{-1}$/cycle	-0.143	-0.028
300 mA/cm2	[mV]	-160.85	-166.16	-160.10	-166.76	µV h^{-1}	16.564	-13.133	µV/cycle	3.589	-2.846
600 mA/cm2	[mV]	-194.59	-205.69	-197.55	-203.04		-65.023	58.161		-14.088	12.602
1000 mA/cm2	[mV]	-219.92	-230.50	-223.27	-231.67		-73.546	-25.784		-15.935	-5.587

Reverse currents

reverse currents		BoL			EoL			Degradation rate							
	Unit	Reverse + 0.4 V	Reverse + 0.7 V	Reverse + 1.1 V	Reverse + 0.4 V	Reverse + 0.7 V	Reverse + 1.1 V	Unit	Reverse + 0.4 V	Reverse + 0.7 V	Reverse + 1.1 V	Unit	Reverse + 0.4 V	Reverse + 0.7 V	Reverse + 1.1 V
io	[mA/cm2]	0.47	0.83	0.43		0.40	0.32	µA $cm^{-2}h^{-1}$		-10.46	-2.13	µA $cm^{-2}h^{-1}$/cycle		-1.73	-0.44
b	[mV/dec]	-47.76	-51.81	-45.39		-60.98	-44.39	µV dec -1 h-1		-221.01	19.49	µV $dec^{-1}h^{-1}$/cycle		-36.65	4.03
CDL	[mF/cm2]	169.20	202.55	176.36		7.24	17.30	mF $cm^{-2}h^{-1}$		-4.71	-3.08	mF $cm^{-2}h^{-1}$/cycle		-0.78	-0.64
1000 mA/cm2	[mV]	-235.34	-224.18	-229.85	-430.78	-434.74	-356.06	µV h^{-1}	-5939.28	-5079.29	-2441.63	µV/cycle	-781.74	-842.26	-504.88
300 mA/cm2	[mV]	-171.77	-156.62	-165.66	-373.67	-359.34	-307.51		-6135.96	-4890.16	-2744.17		-807.63	-810.90	-567.43
600 mA/cm2	[mV]	-206.96	-193.22	-200.07	-435.18	-407.01	-343.18		-6935.44	-5156.92	-2768.38		-912.86	-855.13	-572.44
1000 mA/cm2	[mV]	-232.04	-218.48	-225.40	-453.52	-438.57	-368.70		-6730.87	-5309.12	-2771.96		-885.93	-880.37	-573.18

Clean Hydrogen Partnership Co-funded by the European Union
The project is supported by the Clean Hydrogen Partnership and its members

High currents

High currents		BoL			EoL			Degradation rate			
	Unit	HC 2 A/cm²	HC 3 A/cm²	HC 1 A/cm²	HC 2 A/cm²	HC 3 A/cm²	HC 1 A/cm²	Unit	HC 2 A/cm²	HC 3 A/cm²	HC 1 A/cm²
io	[mA/cm2]	0.51	0.63	0.56	0.55	0.66	0.62	$\mu A\ cm^{-2}h^{-1}$	0.82	0.65	1.19
b	[mV/dec]	-47.95	-47.46	-48.52	-46.43	-48.31	-47.04	µV dec -1 h-1	33.78	-18.64	32.60
CDL	[mF/cm2]	171.10	217.57	178.28	142.79	160.14	159.99	$mF\ cm^{-2}h^{-1}$	-0.63	-1.26	-0.40
300 mA/cm2	[mV]	-166.57	-154.42	-163.91	-172.32	-176.71	-163.73	$\mu V\ h^{-1}$	-127.75	-489.90	3.91
600 mA/cm2	[mV]	-199.96	-190.42	-200.99	-210.13	-217.15	-198.76		-226.02	-587.46	48.89
1000 mA/cm2	[mV]	-224.21	-218.81	-228.58	-235.36	-245.10	-222.28		-247.70	-577.91	138.46

Impurities

Impurities		BoL			EoL			Degradation rate						
	Unit	Imp Reference	Imp Flexibility	Imp On/-50 mA/cm²	Imp Reference	Imp Flexibility	Imp On/-50 mA/cm²	Unit	Imp Reference	Imp Flexibility	Imp On/-50 mA/cm²	Unit	Imp Reference	Imp Flexibility	Imp On/-50 mA/cm²
io	[mA/cm2]	0.48	0.56	0.52	0.40	0.44	0.49	$\mu A\ cm^{-2}h^{-1}$	-1.66	-3.23	-0.77	$\mu A\ cm^{-2}h^{-1}$/cycle	-80.52	-0.32	-0.17
b	[mV/dec]	-52.14	-46.04	-47.57	-41.29	-37.00	-41.32	µV dec -1 h-1	223.99	232.01	137.39	$\mu V\ dec^{-1}\ h^{-1}$/cycle	10849.45	23.13	29.77
CDL	[mF/cm2]	163.76	208.22	161.77	136.92	206.93	179.41	$mF\ cm^{-2}h^{-1}$	-0.55	-0.03	0.39	$mF\ cm^{-2}h^{-1}$/cycle	-26.84	0.00	0.08
300 mA/cm2	[mV]	-177.15	-157.24	-170.18	-128.31	-109.15	-116.98		1008.45	1233.49	1169.23		48846.34	122.98	253.33
600 mA/cm2	[mV]	-212.96	-193.95	-204.63	-156.23	-133.23	-116.98	$\mu V\ h^{-1}$	1171.19	1557.45	1926.40	µV/cycle	56729.27	155.28	417.39
1000 mA/cm2	[mV]	-239.71	-219.23	-228.62	-179.86	-155.62	-163.40		1235.75	1631.72	1433.50		59856.10	162.68	310.59

Clean Hydrogen Partnership Co-funded by the European Union
The project is supported by the Clean Hydrogen Partnership and its members